

Rotational and Translational Motion of Supercoiled Plasmids in Solution

Roger J. Lewis, Janet H. Huang,[†] and R. Pecora*

Department of Chemistry, Stanford University, Stanford, California 94305.
Received August 6, 1984

ABSTRACT: We report dynamic light scattering and transient electric birefringence data on five monodisperse plasmid DNAs ranging in molecular weight from 1.5×10^6 to 8.4×10^6 daltons. The translational behavior closely follows the experimental sedimentation work of Hudson and Vinograd (*Nature (London)*, **221**, 332-7 (1969)) while the apparent rotational relaxation is largely independent of molecular weight, with a decay time around 100-130 μ s at 37 °C ($\Theta = 1280$ -1670 s⁻¹). We attribute this behavior to increasing contributions of internal motions to the overall dynamics, as the plasmids increase in size. An inverse Laplace transform (ILT) analysis can successfully resolve and measure the translational and rotational decays from the light scattering data on the smallest plasmid. These measurements are consistent with a rigid rod 2000 Å in length and 170 Å in diameter. The ILT technique fails, however, to resolve the translational decay from the other relaxations in the data from the larger plasmids.

Introduction

Plasmids, circular pieces of duplex DNA, occur naturally in bacteria¹ and are one of the fundamental tools of recombinant DNA technology.² Naturally existing within bacteria in the supercoiled form,^{3,4} these small genetic units confer resistance to both natural and synthetic antibiotics.¹

For the polymer chemist, however, plasmids have many advantages as a model system for the study of macromolecular dynamics. Because of their importance to genetic engineers and to researchers concerned with bacterial antibiotic resistance, methods for the characterization and manipulation of these polymer molecules are extremely well worked out.² Properly produced, plasmids are absolutely monodisperse⁴ and their molecular weight can often be calculated exactly from existing primary sequence information. Their contour length can also be calculated quite accurately.⁵ Since different researchers can produce plasmid DNAs and be confident that their samples are identical, it is practical to compare results from different laboratories. In addition, there is a large body of related literature on the physical-chemical properties of these molecules in solution.^{6,7} Furthermore, our understanding of the structure-function relationship in DNA is still incomplete.^{8,9} Thus, studies of the motions of these molecules are important to the biologist as well as the polymer chemist.

Discussion

Dynamic light scattering and transient electric birefringence are both useful methods for studying the dynamics of supercoiled and linear DNA.¹⁰⁻¹⁴ In the following work, we have studied the motions of five different supercoiled plasmids by these techniques (see Figure 1). The plasmids ranged in size from 2300 ± 5 base pairs (about 1.5×10^6 daltons) to 12800 ± 400 base pairs (about 8.4×10^6 daltons). The plasmids are monodisperse although there is some uncertainty in their absolute size. The high-angle dynamic light scattering experiments were carried out at 90°, giving a value for q , the scattering vector length, of 2.42×10^5 cm⁻¹. Our low-angle experiments were performed between 10° and 26°, giving correspondingly lower values for q .

At larger values of the scattering vector, the autocorrelation function¹⁵ measured from solutions of these molecules was not a single exponential. Presumably this was due to rotational or internal motions on a length scale

of $1/q$ or greater.¹⁵ Since we were not aware of any reasonable models of superhelical plasmid structure on which to base our data analysis, we used an unbiased, model-independent procedure. CONTIN, a Fortran program written by Provencher,¹⁷⁻¹⁹ can analyze autocorrelation data using a constrained and conditioned inverse Laplace transform (ILT) technique. It finds the smoothest non-negative distribution of decay times that is consistent with the data, to the accuracy in the data.¹⁸⁻¹⁹ No information other than the autocorrelation function itself and the range of possible relaxation times is used by the program. For every plasmid solution, the autocorrelation function measured at 90°, when evaluated by the ILT technique, revealed two relaxation processes (see Figures 2 and 3). The slower of the two, usually with a decay time around 260 μ s, would correspond to the translational diffusion of a spherical particle with a radius of about 500 Å. The faster of the two processes usually had a decay time around 70 μ s. The decay times of both of these processes were surprisingly independent of the molecular weight of the plasmid. Since the ILT technique makes no a priori assumptions with respect to the number of different relaxation processes (translation, rotation, and/or internal motion) that may be contributing to the measured autocorrelation function, we have demonstrated the existence of multiple relaxation processes. In no case were we forced to assume that the multiple relaxation processes did in fact exist and then analyze the data under that assumption.

At low angle, dynamic light scattering is sensitive only to large-scale motions of the scattering particles.¹⁵ This makes low-angle light scattering the method of choice for determining translational diffusion constants of large molecules. Higher scattering angles would make the experimental interpretation more complex because of the increased contribution of internal relaxations to the measured autocorrelation function.¹⁵ At the lower values of q , where we expected only the translational motion of the plasmids to contribute to the light scattering spectrum,¹⁵ experimental limitations made it impossible for us to obtain as accurate data as in the high- q experiments. In these low-angle cases, CONTIN was often inconsistent in its analysis of several different measurements from the same plasmid solution. This was probably because the noise in the data was not Gaussian (it contained a sinusoidal component) and thus the statistical criteria that the program uses internally were invalid.²⁰ For these experiments we analyzed the data with the multiexponential fitting program DISCRETE, also written by Provencher,^{21,22} and we constrained the solution to be a single exponential

[†] Present address: School of Medicine, University of California at San Diego, La Jolla, CA 92093.

with a floated base line. This form adequately represented the data from all the plasmids in the low- q region. The observed single-exponential behavior of the plasmid autocorrelation functions at the low angles confirms the selective measurement of translational diffusion.

The translational diffusion constant is a simple function of the friction constant, f , for the molecule²³

$$D = kT/f \quad (1)$$

where k is Boltzmann's constant, and T is the temperature in kelvin. The sedimentation coefficient, s , is also a simple function of the friction constant¹⁵

$$s = m(1 - \nu\rho)/N_0f \quad (2)$$

where m is the molecular weight, ρ is the density of the solution, N_0 is Avogadro's number, and ν is the mass specific volume. In 1969 Hudson and Vinograd published an empirical relationship between the molecular weight of a superhelical plasmid and its sedimentation coefficient.⁶

$$s = 7.44 + 2.43 \times 10^{-3} m^{0.58} \quad (3)$$

When one uses the equations above and the literature value for ν ,²³ it is possible to calculate the diffusion constant for each plasmid. This sedimentation prediction matches very closely our measured translational diffusion constants. Because sedimentation requires the establishment of a velocity field, there is always the risk that large flexible molecules will "streamline", reducing their frictional constant below the thermal equilibrium value.²³ Because of this, it is not surprising that a small discrepancy develops between the sedimentation predictions and our low-angle measurements as the plasmids increase in size (see Figure 4).

Small, superhelical plasmids are often envisioned as a rodlike quadruple helix. This model makes specific predictions for the light scattering spectrum.¹⁵ Newman has reported work on the motion of pBR322, a plasmid that we use as well. His results are consistent with a rodlike structure up to a moderate value of q .²⁴ Our data on pBR322, to be shown below, are entirely in agreement with Newman's data. Our light scattering data from an even smaller plasmid are consistent with a rigid rod structure at all of our q values. It should be noted, however, that the transient electric birefringence data, even taken from solutions of the smallest plasmid, are not completely consistent with a rigid rod structure. Transient electric birefringence, because it is insensitive to translation, may well be more sensitive to internal motions than dynamic light scattering. Furthermore, the larger plasmids deviated from a rigid rodlike structure to such a degree that they exhibited a rotational motion whose characteristic time is essentially independent of plasmid size, whether measured by dynamic light scattering or by transient electric birefringence.

Experimental Section

Plasmids of five different lengths (Figure 1) were obtained and grown in *E. coli* strain HB101.² Using a minor modification of the procedure of Marko, Chipperfield, and Birnboim,^{30,31} we were able to isolate milligram quantities of plasmid DNA with less than 3% topological contamination (nicked circles and linear molecules) and no detectable RNA or chromosomal DNA. Plasmid solutions (100 μ g/mL in 100 mM NaCl, 10 mM Tris-HCl pH 8.0, 1 mM EDTA) were cleaned of dust by centrifugation in the scattering cell, at 15000g for 15 min and then checked for dust under a microscope during illumination by 0.2 W of 488-nm laser light. When the sample was clean, it was brought to thermal equilibrium at 37 °C and the homodyne dynamic light scattering autocorrelation function was measured; 488-nm laser light from a Spectra Physics Model-165 argon ion laser was used. In a typical experiment, at 90° scattering angle, 512 data points were measured

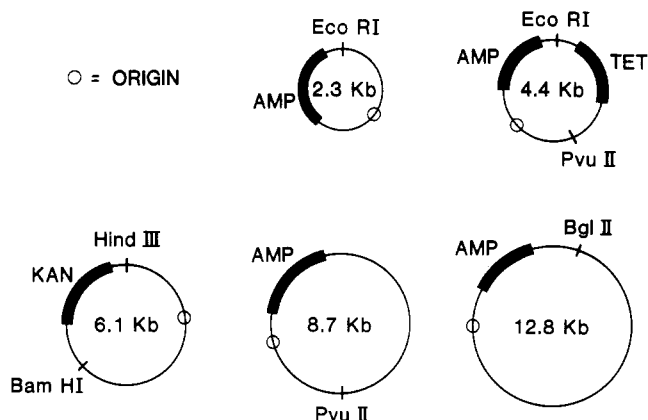


Figure 1. Five plasmids (small autonomously replicating circular pieces of DNA) of lengths 2300 base pairs up to 12 800 base pairs (0.78 μ m up to 4.4 μ m in contour length) are shown diagrammatically. Each contains an origin of replication so that the plasmid may be replicated by the enzymatic machinery of *E. coli*. Each plasmid also contains one or two genes that code for proteins that allow the *E. coli* to resist the toxic effects of various antibiotics. These drug resistance genes allow us to grow large numbers of *E. coli* while positively selecting for the cells that contain the plasmid. The 2.3-, 8.7-, and 12.8-kb plasmids were provided by Thomas Reynolds in the Department of Pathology, Stanford University. Their actual names are pRI25, pSV $\Delta\beta_2$, and pSV $\Delta G_5'$, respectively.²⁵ The 4.4-kb plasmid is pBR322 and the 6.1-kb plasmid is pRLM4.²⁶⁻²⁹ We refer to these plasmids by the number of base pairs to facilitate comparisons between them.

2 μ s apart by using the multiplex capability of a Brookhaven BI2020 autocorrelator. Typical signal to rms noise ratios for these experiments were 500–1000. The data were then spliced together for use with CONTIN. CONTIN was run on a Universe 68 computer, a MC68000-based system manufactured by Charles River Data Systems. Both before and after the scattering experiment the DNA was analyzed for nicking by agarose gel electrophoresis.² Less than 5% of the DNA was nicked after the experiments.

Transient electric birefringence measurements were made on 5 μ g/mL solutions of DNA in 1 mM sodium phosphate buffer pH 7.0 at 4.3 °C; 1000 100-V orienting pulses of width 50 or 150 μ s were applied at 5-Hz repetition rate; 2048 data points 640 ns apart were measured. Single-exponential fits were performed by linear regression to the log transform of the data, using points from 50 to 300 μ s. The signal before the pulse was used as the base line. This work was performed at the laboratory of and with the help of Don Eden of San Francisco State University, using apparatus described previously.¹²

Electron microscopy was performed by using standard cytochrome *c*/uranyl acetate/Pt staining.³² This work was aided by Arnold Barton.

Results

We have modified CONTIN so that it displays the values of relaxation times in terms of the size of a spherical particle whose translational decay would have the same decay time. We call this the "effective hydrodynamic radius" for the decay process. This is useful when attempting to sort translational from other relaxation processes in a system, as the position of a translational peak will not change with angle using this system, whereas a rotational peak will. If relaxation times themselves were plotted, positions of both kinds of delay processes would change with angle.

Very often a peak appears at the smallest radius (fastest time scale) made available to the program, even when using computer-synthesized data that contain no decay time near that region.²⁰ These peaks will move in position as the lower size limit is changed and they rarely represent more than 2% of the scattered light. They are an artifact whose cause is unknown to us. They seem to have little or no effect on the solution chosen by the program, as long as

Angular Dependence of Spectra from 2.3 Kb Plasmid

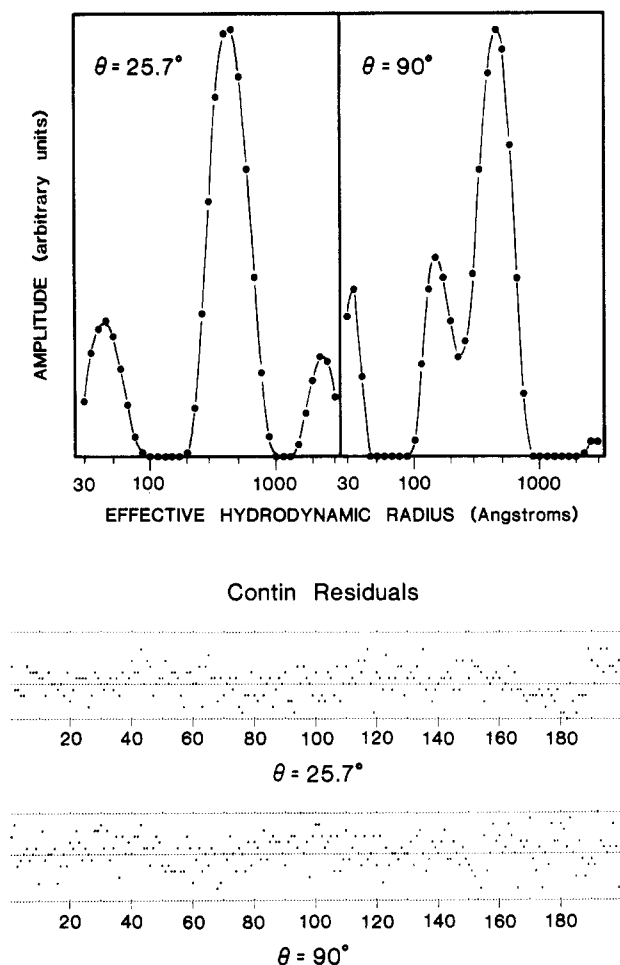


Figure 2. This figure shows CONTIN analyses of light scattering data from solutions of the 2.3-kb plasmid, taken at 25.7° and 90°. In the first panel, taken at the lower angle, there are three peaks. The fastest decay process, which corresponds to the smallest effective hydrodynamic radius, is at about 45 Å. This is probably an artifact (see text) and represents less than 2% of the scattered intensity. The middle peak, at 430 Å, represents the translational diffusion of the plasmid and contains about 60% of the scattered amplitude. The third peak, at about 2500 Å, is a "dust peak" commonly seen in inadequately cleaned samples at high angle, or in almost all samples at low angle. It contains the rest of the scattered amplitude. The second panel shows the analysis of data taken at 90°. In addition to the probable artifact at 35 Å (less than 1% of the scattered intensity) and the dust peak at the large end of the spectrum (about 10% of the scattered intensity), there are now two peaks near the center of the spectrum. The slower of the two peaks, now at about 460-Å effective hydrodynamic radius, represents translation. The faster of the two peaks, at about 160-Å effective hydrodynamic radius, represents rotational and/or internal motion in the plasmid. The bottom section of the figure shows plots of weighted residuals vs. channel number from the two fits shown above. Both sets of residuals are statistically random by a nonparametric sign test.

they are reasonably removed from the actual decay times that exist in the system.²⁰

Figure 2 shows the CONTIN analysis of data taken from solutions of the smallest plasmid at two scattering angles. At 25.7° we expected only the translational motion of the molecule to contribute to the autocorrelation function and CONTIN's analysis revealed only one significant relaxation process. The position of the relaxation at 430-Å effective hydrodynamic radius agrees reasonably well with 400 Å predicted for translational diffusion by the previously mentioned sedimentation measurements. At 90° scattering angle, rotational and/or internal motions of the molecule

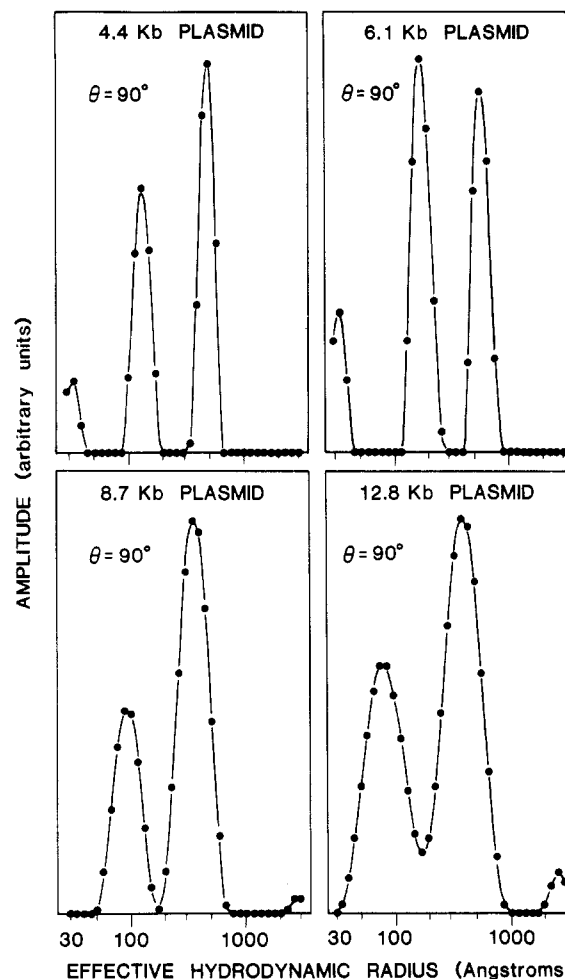


Figure 3. This figure shows CONTIN analyses of light scattering data from solutions of each of the larger plasmids, each taken at 90°.

can contribute to the autocorrelation function. CONTIN's analysis of these data shows two significant peaks. The slower of the two, presumably representing translational diffusion, is at 460 Å, essentially in the same position as in the low-angle analysis. The peak at 160 Å (approximately 80-μs decay time) represents some sort of faster motion, either rotation or flexing of the molecule (or both). In the case of the smallest plasmid, CONTIN is able to resolve the translational motion of the molecule from some other, faster motion and accurately determine the translational relaxation time.

Figure 3 shows CONTIN analyses of 90° scattering data taken from each of the larger plasmids. Despite the increasing size, and the associated proliferation of possible internal motions, the spectra look surprisingly similar. The only indication of increasing complexity is the broadening of the peaks with increasing molecular weight. The peak width of bimodal decay time distributions is difficult to measure and this observation may or may not be significant.¹⁶

How compatible are these results with the known structure of these plasmids? Starting with the smallest plasmid, we see that the slow decay time very closely matches the sedimentation prediction for translational diffusion. How reasonable is the rotational time? The autocorrelation function for a rigid rod has the form¹⁵

$$g(t) = S_0(q) \exp(-q^2 D t) + S_1(q) \exp[-(q^2 D + 6\theta)t] + \dots \quad (4)$$

The faster time, 80 μs, actually represents the addition of

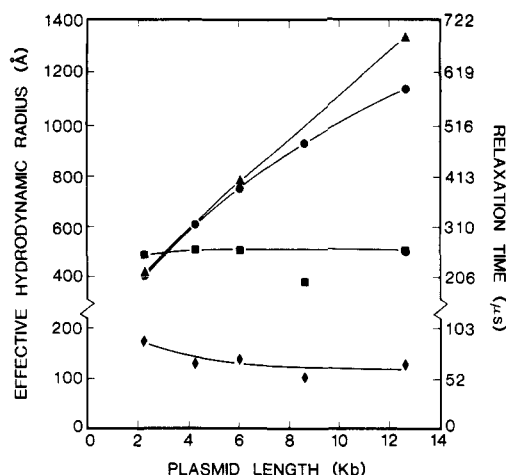


Figure 4. This figure summarizes the light scattering results and compares the low-angle results with predictions based on previously published sedimentation data. Each point represents the average from at least two experiments. The circles show the translational relaxation times that are predicted from previously published sedimentation measurements on similar molecules.⁸ The triangles show the single relaxation time that was observed at low angles for all of the plasmids. Presumably this was due to the translational motion of the plasmids. The squares show the slower of the two relaxation processes observed by light scattering at 90° and the diamonds show the faster of the two.

the translational and rotational decay constants, as seen in the second term. Using the translational time of 206 μ s (obtained by averaging our values for D from the low-angle measurements and scaling by q^2) and the measured rotational time of 80 μ s yields a true rotational time ($1/6\theta$) of 130 μ s. It is reassuring to note that transient electric birefringence measurement of an average rotational time for this plasmid, when scaled by the difference in temperature and viscosity of water at 4.3 and 37 °C,³³ yields a time of 98 μ s. This is in surprising agreement given the different ionic strengths and temperatures used in the two experiments. Using Broersma's relations³⁴⁻³⁶ and the simple model of a rigid rod 2000 Å in length and 170 Å in diameter, we would predict a translational time of 207 μ s and a rotational time of 130 μ s at 37 °C. A calculation of ql , the product of the scattering vector and the rod length, gives 1.5 at 25.7° and 4.8 at 90°, confirming our assumptions about the magnitude of the form factors ($S_0(ql)$ and $S_1(ql)$) at the two angles.¹⁵ Thus, the data from light scattering and transient electric birefringence agree and support the rigid-rod model for the smallest plasmid.

For the larger plasmids the picture becomes more confusing (see Figure 4). If we blindly assume that the slow peak continues to represent translation and the faster peak represents rigid rotation, then we are forced to conclude that the translational and rotational diffusion constants for plasmids are surprisingly independent of molecular weight. This is in direct conflict with the sedimentation predictions for the translational diffusion constant.

The data from low-angle scattering experiments, fitted to a single exponential, demonstrate that the translational motion did indeed become slower as the plasmids increased in size. One possible explanation for CONTIN's failure to detect this is that the larger plasmids, with additional bending or rotational modes, might possess too complex a dynamic spectrum. If the data were of insufficient accuracy to resolve all of the relaxation times, CONTIN might have combined the translational motion and some other faster relaxation process into one peak. In this case the position of the observed slower peak would be faster than the actual translational time and probably slower than the

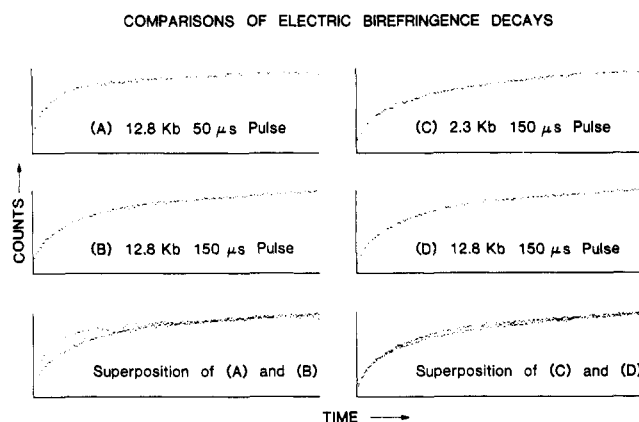


Figure 5. This figure shows the zero-field transient electric birefringence decay of the smallest and largest plasmids as measured in the laboratory of Don Eden. The time scales are the same in each panel. In the first set of panels are data taken from solutions of the 12.8-kb plasmid using two different orienting pulse widths, 50 and 150 μ s in panels A and B respectively. By superimposing the two decays in the third panel on the left side, we can see that the two decays are different. This is confirmed by single-exponential fits to the data. A similar result was seen in the case of the 2.3-kb plasmid. This suggests that there are at least two different rotational decay processes that have different decay times. Presumably one is rotation of the entire molecule and the others are internal bending modes. In the right-hand set of panels we compare data from the 2.3- and 12.8-kb plasmids, each taken with a 150- μ s orientation pulse. The striking feature is that the rotational decay of the smallest plasmid (panel C) and the rotational decay of the largest plasmid (panel D) are nearly superimposable (last panel). This confirms that the apparent rotational motion of the plasmids is essentially independent of the contour length over the range we have studied. The values for the rotational times of the molecules as measured by this technique agree quite well with the values from light scattering (see text).

relaxation time of the additional "hidden mode". On the other hand, CONTIN's failure might not have been a failure at all. It is possible that the form factor¹⁵ for the translational relaxation became so small as the plasmids became larger that, in effect, no translational information is contained in the 90° autocorrelation function. In this case the slower of the two resolved peaks might represent the first internal mode of the plasmids.

We performed transient electric birefringence measurements on the 2.3-, 6.1-, and 12.8-kb plasmids. The average zero-field relaxation decay times for these plasmids were 98, 102, and 96 μ s, respectively. These values, although the experiments were performed at 4.3 °C, have been corrected to 37 °C by dividing by the ratio of the viscosity of water at the two temperatures³³ and then scaling by the absolute temperatures. The molecular weight independence of these times confirms the 90° light scattering results.

These times are averages of at least two decay processes as, even in the case of the smallest plasmid, the decays were not single exponential (see Figure 5 for an example; the 2.3-kb data are not shown). This lends support to Newman's statement²⁴ that the rigid-rod model, in the case of pBR322, "fails at higher angles, probably due to ... flexibility or branching...."

There are two possible explanations for the existence of an apparent rotational motion that is independent of the contour length of the DNA. One possibility is that the larger plasmids are more densely packed structures in solution than the smaller plasmids, so that their overall rotational friction is not affected by their increased contour length. A second possibility is that, in the case of the smallest plasmid, the motion is a rotation of the entire

MEASUREMENT OF PLASMID DIMENSIONS BY ELECTRON MICROSCOPY

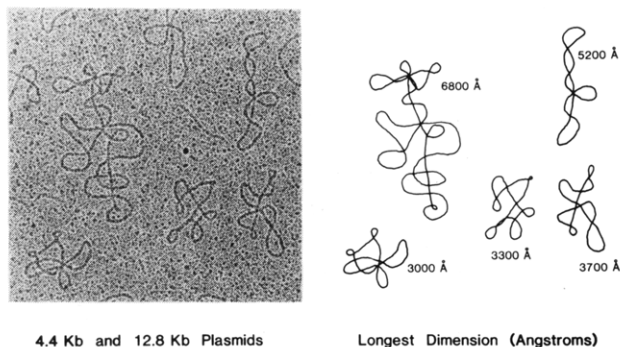


Figure 6. This figure shows a section of an electron micrograph containing one of the 12.8-kb plasmids and four of the 4.4-kb plasmids. The length of the longest dimension of each plasmid is shown to the right.

plasmid while in the case of the larger molecule it may be a rotation of only a part of the molecule.

Electron microscopy has historically been used to characterize the structure of nucleic acids. Figure 6 shows an electron micrograph of the 4.4- and 12.8-kb plasmids. We measured the longest dimension of the plasmids to see if the 12.8-kb plasmid did in fact have a larger longest dimension. After measuring approximately a dozen of each plasmid, we concluded that, on the average, the longest dimension of the 12.8-kb plasmid is about twice as long as the longest dimension of the 4.4-kb plasmid (0.76 ± 0.06 vs. $0.37 \pm 0.05 \mu\text{m}$). Thus, the larger molecules do not appear to be more densely packed structures than the smaller ones, at least by this technique. Uncertainties in the extent of distortion occurring during the spreading of the molecules often preclude drawing conclusions from electron micrographs.²³ Nonetheless, we suggest that the rotational motion observed by light scattering and transient electric birefringence is a rotation of only a part of the larger molecules. In the case of the smallest plasmid it might well represent a rotation of the entire molecule.

Acknowledgment. This work was supported by NIH Grant 2ROI GM 22517 and NSF Grant CHE 82-00512 and the NSF MRL Program through the Center for Materials Research at Stanford University. R.J.L. was supported by the NIH Medical Scientist Training Program at the Stanford University School of Medicine.

References and Notes

- (1) Jawetz, E.; Melnick, J. L.; Adelberg, E. A. "Review of Medical Microbiology"; Lange Medical Publications: Los Altos, CA, 1980.

- (2) Maniatis, T.; Fritsch, E. F.; Sambrook, J. "Molecular Cloning, A Laboratory Manual"; Cold Spring Harbor Laboratory: Cold Spring Harbor, NY, 1982.
- (3) Bauer, W. R.; Crick, F. H. C.; White, J. H. *Sci. Am.* **1980**, *243*, (1), 118.
- (4) Kornberg, A. "DNA Replication"; Freeman: San Francisco, CA, 1980.
- (5) Dickerson, R. E. *Sci. Am.* **1983**, *249* (6), 94.
- (6) Hudson, B.; Vinograd, J. *Nature (London)* **1969**, *221*, 332.
- (7) Upholt, W. B.; Gray, H. B., Jr.; Vinograd, J. *J. Mol. Biol.* **1971**, *61*, 21.
- (8) Miller, J. H.; Reznikoff, W. S. "The Operon"; Cold Spring Harbor Laboratory: Cold Spring Harbor, NY, 1980; pp 221-43.
- (9) Kolata, G. *Science* **1984**, *224*, 1228.
- (10) Pritchard, A. E.; O'Konski, C. T. *Ann. N. Y. Acad. Sci.* **1977**, *303*, 159.
- (11) Campbell, A. M.; Jolly, D. J. *Biochem. J.* **1973**, *133*, 209.
- (12) Elias, J. G.; Eden D. *Macromolecules* **1981**, *14*, 410.
- (13) Hagerman, P. J. *Biopolymers* **1981**, *20*, 1503.
- (14) Voordouw, G.; Kam, Z.; Borochoy, N.; Eisenberg, H. *Biophys. Chem.* **1978**, *8*, 171.
- (15) Berne, B. J.; Pecora, R. "Dynamic Light Scattering"; Wiley: New York, 1976.
- (16) Bott, Steven E. Ph.D. Thesis, Stanford University, Stanford, CA, 1984.
- (17) Provencher, S. W.; Hendrix, J.; De Maeyer, L.; Paulussen, N. *J. Chem. Phys.* **1978**, *69*, 4273.
- (18) Provencher, S. W. *Makromol. Chem.* **1979**, *180*, 201.
- (19) Provencher, S. W. "CONTIN User's Manual", Technical Report EMBL-DA02; European Molecular Biology Laboratory; Heidelberg, 1980.
- (20) Bott, Steven E., personal communication.
- (21) Provencher, S. W. *Biophys. J.* **1976**, *16*, 27.
- (22) Provencher, S. W. *J. Chem. Phys.* **1976**, *64*, 2772.
- (23) Cantor, C. R.; Schimmel, P. R. "Biophysical Chemistry"; Freeman: San Francisco, CA, 1980.
- (24) Newman, J. *Biopolymers* **1984**, *23*, 1113.
- (25) Reynolds, Thomas C., personal communication.
- (26) Bolivar, F.; Rodriguez, R. L.; Greene, P. J.; Betlach, M. C.; Heyneker, H. L.; Boyer, H. W.; Crosa, J. H.; Falkow, S. *Gene* **1977**, *2*, 95.
- (27) Sutcliffe, J. G. *Nucleic Acids Res.* **1978**, *5*, 2721.
- (28) Sutcliffe, J. G. *Cold Spring Harbor Symp. Quant. Biol.* **1979**, *43*, 77.
- (29) Wold, M. S.; Mallory, J. B.; Roberts, J. D.; LeBowitz, J. H.; McMacken, R. *Proc. Natl. Acad. Sci. U.S.A.* **1982**, *79*, 6176.
- (30) Marko, M. A.; Chipperfield, R.; Birnboim, H. C. *Anal. Biochem.* **1982**, *121*, 382.
- (31) Clewell, D. B. *Bacteriology* **1972**, *110*, 667.
- (32) Davis, R. W.; Simon, M.; Davidson, N. *Methods Enzymol.* **1971**, *21*, 413.
- (33) "Handbook of Chemistry and Physics"; CRC Press: Boca Raton, FL, 1979.
- (34) Broersma, S. *J. Chem. Phys.* **1960**, *32*, 1626.
- (35) Broersma, S. *J. Chem. Phys.* **1960**, *32*, 1632.
- (36) Newman, J.; Swinney, H. L.; Day, L. A. *J. Mol. Biol.* **1977**, *116*, 593.